Real-time Detection of Earthquake Swarms at Redoubt Volcano, 2009

Glenn Thompson and Michael E. West
Geophysical Institute and Alaska Volcano Observatory, University of Alaska Fairbanks

BACKGROUND

Alarm systems can play a critical role in alerting scientists to anomalous seismicity such as earthquake swarms and volcanic tremor that often precedes or coincides with explosive volcanic eruptions or dome failures. By reducing the need for visual data monitoring, a reliable alarm system can also be a cost effective way to monitor seismicity and minimize fatigue of volcano observatory staff during a prolonged period of volcanic unrest. Recognizing this we designed and implemented a real-time earthquake swarm alarm system capable of identifying the start of, escalations during, and end of a swarm. This system was used to monitor seismicity throughout the 2009 eruption of Redoubt volcano.

INTRODUCTION

The Alaska Volcano Observatory (AVO) seismically monitors 31 volcanoes in the Alaska Peninsula and Aleutian Islands. Twice-daily checks of web-based digital helicorder plots, spectrograms and reduced displacement plots (Benoit *et al.* 1998) are designed to catch the onset of volcanic unrest. Even such a strict regimen has weaknesses. Pavlof volcano erupted on 16 September 1996, surprising scientists. Seismologists reprocessed seismic data and found several hours of precursory tremor on 11 September that had been masked by storm noise (McNutt 2002). Pavlof erupted again on 14 August 2007, with little precursory seismicity (Waythomas *et al.* 2008). On 12 July 2008, Okmok volcano erupted with less than five hours of precursory seismicity sending ash to 50,000 feet (Larsen *et al.* 2009). A short-lived swarm was the sole seismic precursor. There was no precursory tremor. Although such a rapid onset is uncommon, it highlights the need for alarm systems that can alert scientists to volcanic tremor and earthquake swarms.

Despite this, little has been published about volcano-seismic alarm systems. The most familiar is probably the Real-time Seismic Amplitude Measurement (RSAM) alarm system. Although this is part of the popular RSAM system (Murray and Endo 1992), the alarm module was never described (Thomas L. Murray, personal communication 2009). It allows event and tremor alarms to be defined, based on RSAM thresholds, and sent by modem to landline telephones. This system was installed as part of a portable PC-based seismic monitoring system by the Volcano Disaster Assistance Program (VDAP) in developing world volcano observatories (*e.g.,* Murray *et al.* 1996), and is also used at U.S. volcano observatories. It later became a component of the VDAP Glowworm system (Marso *et al.* 2003a), with modem alarms replaced by SMS/email alarms. One of the authors (G. T.) used the RSAM alarm system extensively at the Montserrat Volcano Observatory (MVO) between 2000 and 2003, where it provided warnings about hundreds of pyroclastic flows as they developed, and before they threatened populated areas or regional aviation. It is still used at MVO today (Roderick Stewart, personal communication 2009), and was used to monitor the 2003 eruption of Anatahan volcano (Marso *et al.* 2003b), and the 2004 eruption of Mt. St. Helens (Qamar *et al.* 2008). The RSAM system has inspired other tremor alarm systems, including a Web-configurable reduced displacement alarm system (Aki and Koyanagi 1981; Benoit *et al.* 1998; Thompson and West 2009).

While the RSAM system is a highly effective tool for monitoring volcanic tremor and isolated events, it does not provide a mechanism to monitor earthquake swarms (Thomas L. Murray, personal communication 1999). While it does include a simple short-term average (STA) to long-term average (LTA) algorithm to count the number of single station detections, it does not count events, nor can it be configured to send alarms based on detection rate. Our goal in this paper is to describe a new type of volcano-seismic alarm system: one for tracking earthquake swarms.

Benoit and McNutt (1996) define a volcanic earthquake swarm as a sequence of events, closely clustered in time and space without a single outstanding shock, that occur within about 15 km of a volcano, and represent a significant increase in the rate of local volcanic earthquakes above the background rate. We adopt the term "swarm episode" to refer to one or many swarms that cluster closely in time without the seismicity returning to background levels in between.

In addition to swarm onsets, we also wanted to identify increases in swarm activity and the end of swarms. Swarms may intensify through an increase in rate and/or magnitude, so our system is designed so it can detect increases in rate, in magnitude, or in both. According to the Generic Volcanic Earthquake Swarm Database (Benoit and McNutt 1996), 34% of swarms end prior to a volcanic eruption (23% immediately before), so the end of a swarm may be a better predictor for

doi: 10.1785/gssrl.81.3.505

eruption than the start of a swarm. Additionally, STA/LTA detection algorithms break down in the presence of vigorous seismic tremor or when events are too close together in time to be detected, causing the event detection rate to drop sharply when the seismicity is actually increasing. Thus an (apparent) end of a swarm could signal an imminent explosive eruption.

We describe an earthquake swarm alarm system implemented at the Alaska Volcano Observatory shortly before the 2009 eruption of Redoubt volcano. The extended eruption sequence provided an unparalleled live test of the system. Swarm alarms were successfully sent during all major seismic swarm episodes. Swarm episodes from 21–23 March and 2–4 April immediately preceded the first and last of 19 explosive eruptions that sent ash to elevations of up to 20 km. The primary components of the system, detailed below, include: a generic real-time earthquake detection and location system; a swarm tracking system which contains the detection logic, and a smart notification system that couples a progressive cell phone and e-mail call-down mechanism with a Web interface and database to track the alarm history and user interaction.

THE REAL-TIME EVENT CATALOG

The critical input for the swarm alarm system is a real-time earthquake catalog. This catalog provides the event list, magnitudes and locations that are monitored for changes. Most seismic networks operate one or more forms of earthquake detection using production software packages such as Earthworm (Bittenbinder *et al.* 1994), Antelope (Harvey 1999) or SeisComP3 (Weber *et al.* 2007). The real-time catalog used here is built on Antelope. Though the swarm alarm makes extensive use of the Antelope code base as well, the methodology is fully transferable. This catalog is separate from AVO's analyst-reviewed catalog which is produced using the XPick interactive picking program (Robinson *et al.* 1991) and the Hypoellipse location package (Lahr 1989). Though the event locations and magnitudes in the analyst-reviewed catalog are far superior, the delay required for manual review renders this catalog unsuitable for rapid notification.

The preparation of the real-time earthquake catalog consists of several stages. In the first stage, a standard STA/LTA detector (ratio of short term average to long term average) operates on continuously arriving data filtered into two frequency bands. The higher frequency band (3–25 Hz) is designed to detect high frequency volcano-tectonic earthquakes. A lower frequency band (0.8–5.0 Hz) is tuned to be more responsive to low-frequency earthquakes.

Phase detections are then associated via grid search with likely earthquake hypocenters. Each volcano appears in three separate hypocenter search grids, which we refer to as the regional, local, and vicinity grids. The regional grid matches detections over a wide geographic region (a few hundred kilometers or more) and requires many P and S detections to fit a hypocenter. If an event successfully associates on the regional grid, it is considered the best fit.

The local grid spans a few tens of kilometers centered on the volcano. For a typical Aleutian volcano we require four or five detections to successfully associate with travel time errors of less than 1.0 s. At such close range P and S arrivals are often separated by just a fraction of a second. The same reasons that make S waves a powerful constraint on locations permit incorrect S picks to grossly corrupt hypocenter solutions. For this reason we do not currently use S waves for automated locations on local hypocenter grids. This may change as more sophisticated phase detectors come into use.

The final grid search uses a concept we refer to as a vicinity grid. It is the same as the local grid except that it contains just a single point at the location of the volcano and has an allowable phase pick error of 3 s. Though this error is too large to permit reliable locations, it is sufficient to determine that some sort of event has occurred. It is a catch-all network trigger for detecting events that are significant enough to be monitored, but do not meet the basic quality standards required for location on either the local or regional grids. This is important for low-frequency events which are generally more emergent and have correspondingly more error in their detection times and subsequent locations. Unlike single-station counting methods, the vicinity grid approach is reasonably robust to changes in the network configuration. The vicinity criteria allow us to extend our monitoring to lower magnitude ranges and include more low frequency and rockfall type events. For algorithms such as swarm detection, which are specifically sensitive to the rate of earthquakes, judicious inclusion of these events will improve the sensitivity of the system.

Vigorous swarms at Redoubt were logged with a median catalog latency of 30 s. When the interevent time dropped below 11 s (rates of ~300 events/hr), event detection broke down as new events arrived before the coda of the previous event had decayed sufficiently. Techniques that make use of waveform correlation or wavelets to identify detections would increase the performance somewhat. However, the problem of associating detections with suitable hypocenters is considerably more tractable when the time between earthquakes is greater than the travel time across the array.

Associating each earthquake with its grid criteria provides a basis for subsetting different categories of events for specific uses. For example, vicinity events should not be used in cumulative magnitude calculations. Distant regional events should not be included in volcanic swarm.

The swarm alarm system, described below, is independent of the method used to produce the input catalog. The separation of the catalog production from the swarm detection and alarm management modules is one of the key design concepts. Modules are linked only by shared database tables. Decoupling these modules allows them to be upgraded independently of one another. The real-time earthquake processing, in particular, can be improved considerably by incorporating more sophisticated phase detectors, velocity models and relative relocation capabilities. Parts of the system could even be farmed out entirely to other regional or global seismic networks. So long as a unified catalog is produced in near real-time, the swarm alarm system does not even need to know about these changes.

THE SWARM TRACKING SYSTEM

Metrics

The central problem of swarm detection is how to define the start, escalation, and end of a swarm in an automated algorithm. The event rate may slowly increase (or decrease) over a period of several hours, eventually creeping above (or below) a preset threshold. When the first event is recorded, it is not possible to know that it is the first event in a swarm, nor how long the swarm will be. Nor is it possible to know if an event is the last in a swarm. We accept this ambiguity and realize that a swarm system needs to be configurable based on seismicity patterns, the seismic network, and the needs of the organization.

Many authors have considered approaches for characterizing earthquake swarms in retrospective analysis (*e.g.,* Chouet *et al.* 1994; Benoit and McNutt 1996; Neuberg *et al.* 2000; Rowe *et al.* 2004). Though our real-time focus precludes most of these techniques, our objective is straightforward. We are less concerned with defining the most scientifically appropriate swarm start time, and more interested in alerting network operators when the rate of earthquakes is sufficiently elevated to warrant additional analysis and/or warnings to emergency managers. Because of the variation inherent in swarm classification and the different needs of network operators, there are few universal swarm parameters. Here we treat swarm detection less as a study of intrinsic properties and more as an empirical engineering study.

To achieve the flexibility required for use in a wide range of seismic settings, we base our swarm tracking on four intuitive metrics. These metrics are continuous functions of time calculated on the fly from parameters in the real-time earthquake catalog:

- *mean_rate*: the average number of events per unit time. This metric has long been a staple of most volcano monitoring regimen. Though often presented in events/hour or events/day, this metric can be computed on an arbitrary time base. It is simple to understand, and shows swarms clearly.
- *median_rate*: the reciprocal of the median time between events. This is always greater than *mean_rate*. It is particularly useful for detecting abrupt changes in event rate, as it is more sensitive than *mean_rate*.
- *mean_ml*: the mean M_L (local magnitude) of all events within a time window. This metric allows alarms to be sent if the average size of events increases. It also allows swarms comprised of very small earthquakes to be ignored, if that is desired.
- *cum_ml,* the cumulative M_L of all events within the time window. The cumulative magnitude of a sequence of earthquakes is the sum of the energy of all those events, expressed as a magnitude. This enables alarms to be sent if the energy release rate of a swarm increases. It also allows weak swarms to be ignored, if desired. Appendix A describes how *cum_ml* is computed.

In many cases, simple uses of *mean_rate* will suffice. However, during extended periods of volcanic unrest, which are typically accompanied by frequent earthquake swarms, these simple metrics provide the logic suitable to construct more finely-tuned notifications. If specific patterns are known to have more serious hazard implications, this framework allows other types of behavior to be filtered out.

For example, we could require a *mean_rate* threshold of 20 and a *cum_ml* threshold of 2.5. In this case even if there were 100 events with $M_L = 0.5$, they would not trigger an alarm because *cum_ml* would only be 1.8 (Appendix A). This functionality is useful, for example, during extended dome building sequences such as that in 2004 at Mt. St. Helens (Moran *et al.* 2009) where a background of steady small magnitude earthquakes would have otherwise saturated the *mean_rate* metric.

A very different sensitivity is required in areas of low background seismicity. Prior to the 2008 Okmok eruption (see introduction), background seismicity was no more than a few small earthquakes per day. In this situation, the minimum time window for calculating a meaningful *mean_rate* might be eight hours. To preserve sensitivity to short bursts of seismicity, a low *mean_rate* threshold, perhaps one event/hr, can be coupled with a *median_rate* threshold of six events/hr. In this case six events could occur in six hours without declaring an alarm. However, if four of these events occurred in a half hour, the alarm would be declared.

At a regular time interval (seconds to minutes) the event catalog is subsetted for events that occur within the current time window and are on the local or vicinity grids for a particular volcano (events on the regional grid are ignored). The four metrics are computed and checked against thresholds which define the transition between different states. An alternative method is to compute the metrics each time a qualifying event is added to the catalog. Though we originally employed this technique, we were unable to detect the end of swarms because it did not run when events ceased.

DETECTION OF SWARM STATES

The three possible states are: 1) a swarm is happening, but has not escalated; 2) a swarm is happening and has escalated one or more times; 3) no swarm is happening. Transitions between states occur by comparing metrics against pre-defined thresholds. Each time there is a transition an alarm is declared and the metrics are recorded in the alarm database together with a text message containing the pertinent swarm statistics (to be dispatched by the alarm management system). The new state is also recorded.

If no swarm is happening, the only transition that can occur is the start of a new swarm. A pre-defined "swarm_start" threshold sets a minimum value for *mean_rate*, and can also set minimum values for *median_rate*, *mean_ml* and/or *cum_ml*. The simplest threshold would just consist of an expression for *mean_rate*, *e.g., mean_rate* ≥ 20.

If a swarm is occurring (regardless of whether or not it has escalated), it can either escalate (further), or end. A "significant change" threshold is used which can define a minimum change in *mean_rate* and optionally other metrics. A swarm is deemed

Subject: 'Swarm Over Redoubt 22:13:00 AKDT'
2009/03/23 6:13:00 UTC
Span: 60 minutes
Evts: 14 (14 located)
Mean Rate: 13/hr
Median Rate: 17/hr
Mags: 0.2/0.9/1.6 (of 13)
Cum Ml: 1.9
RDN(12) REF(11) NCT(10) RSO(7) DFR(6) RDJH(6) RED(4) RDWB(0)
End.

Confirm at: www.avo.alaska.edu/internal/confirm_alarms.php

▲ **Figure 1.** Example alarm message generated by the swarm tracking system and dispatched to a call-down list by the alarm management system. It shows the time window length (span), number of events, mean rate, median rate, minimum, mean and maximum magnitudes, cumulative magnitude and how many arrivals a particular station received within the time window. It also provides a clickable link for the recipient to acknowledge the alarm and cancel the call-down. The message can also be viewed via a link from the alarm acknowledgement web page.

to have escalated when metrics are a "significant change" above the swarm_start alarm threshold, *i.e.,* the swarm intensity has significantly increased since it began. For example, in the above case if the significant change *mean_rate_ratio* = 2, an escalation alarm would be declared when *mean_rate* ≥ 40.

A swarm is deemed to have ended when the metrics show a significant change below the new alarm threshold, *i.e.,* the swarm intensity has significantly decreased since it began. For example, if the swarm_start threshold is *mean_rate* ≥ 20, and the significant_change *mean_rate_ratio* is 2, then a swarm_end will only be declared when *mean_rate* ≤ 10.

If metrics significantly increase over the escalation alarm threshold, a second escalation alarm is declared. For example, in the above case if *mean_rate* ≥ 80, a second swarm_escalation alarm would be declared. A third escalation alarm would be sent if *mean_rate* ≥ 160, and so on. This provides a mechanism to alert scientists to swarms that keep intensifying.

Finally, our swarm tracking system can provide reminders of an ongoing swarm. If a swarm is continuing, but no alarm has been sent about it within a configurable timeframe (*e.g.,* six hours), a reminder alarm is declared. We did not use this feature during the Redoubt eruption, though it could be useful during prolonged swarms such as those at Mt. St. Helens in 2004 (Moran *et al.* 2008).

DISPATCHING AND ACKNOWLEDGING ALARMS

A generic alarm management system continuously monitors the alarm database for new alarms, and dispatches each new alarm message (Figure 1) to recipients defined in a call-down list. Each recipient is configured with an email address (including cell phone and pager addresses) and a delay time. The delay time is the number of seconds to wait before wait before dispatching the message to the recipient. By configuring the delay times to increase for each recipient on the list, the notification progress becomes an iterative call-down, instead of a mass broadcast. The call-down can be terminated by acknowledging the alarm through a web interface which tags the alarm in the database with the acknowledgement and the responding user's name. The call-down log for each alarm is also recorded in the database (and shown on the web interface), providing a clear record of alarm response (Figure 2). In many cases only the first recipient will receive the alarm message, because they cancel the alarm before it is dispatched to the next recipient.

Time (UTC)	Recipient	Delay (s)
2009/03/23 6:14:15	seis_alarms@avo.alaska.edu	15
2009/03/23 6:14:16	glennthompson197@gmail.com	74
2009/03/23 6:16:29	9074747424@mms.att.net	207

This alarm was acknowledged by jpdixon at 2009/03/23 06:19:24 UTC

▲ **Figure 2.** Example alarm call-down generated by the alarm management system. This information can be viewed via a link from the alarm acknowledgement webpage.

Several problems could prevent a recipient acknowledging an alarm in a timely fashion, *e.g.,* they might not hear the alarm, might be unable to respond, or might be out of cellular phone range. The call-down list allows users to "pass" the responsibility when necessary. However it also applies a social pressure to respond quickly before subsequent recipients are disturbed. The primary responder—the AVO Duty Seismologist—changes weekly.

THE 2009 ERUPTION OF REDOUBT VOLCANO

We demonstrate the performance of the swarm alarm on earthquake data from the 2009 eruption of Redoubt volcano. Because earthquake catalogs record only discrete events and do not capture the sustained seismicity characteristic of volcanic tremor and explosive eruptions, we supplement the swarm information with reduced displacement. Reduced displacement is a measure of the time-averaged characteristic amplitude of continuous seismic waveforms. It is similar to RSAM (Murray and Endo 1992). Unlike RSAM, which has units of digital counts, reduced displacement data are instrument corrected, integrated to displacement, and then have a geometrical spreading correction applied so that they can be meaningfully compared from one station to another, and from one volcano to another. Empirical relationships exist linking reduced displacement with ash column heights and the Volcano Explosivity Index (McNutt 1994).

The AVO algorithm measures the surface-wave reduced-displacement (D_{RS}) and assumes tremor is mainly comprised of surface waves, which attenuate less with distance than body waves. The value recorded corresponds to the median of the

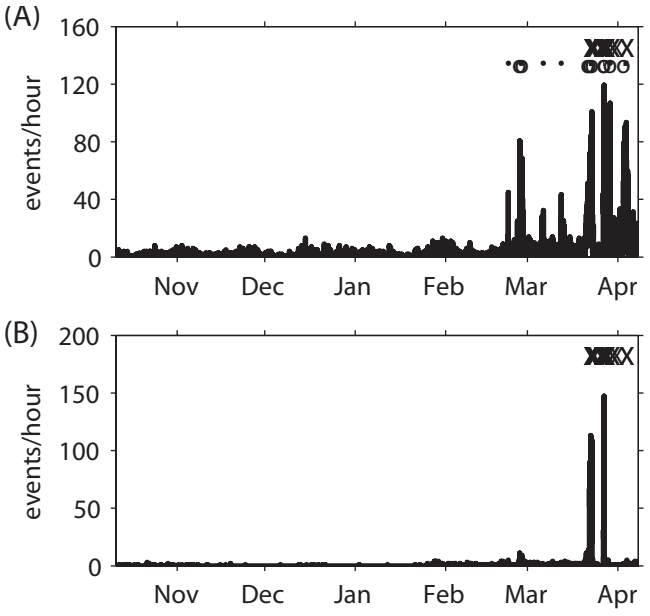

▲ **Figure 3.** Summary of seismicity at Redoubt volcano from 10 October 2008 to 8 April 2009, and alarms sent. A) The number of events per hour declared by the real-time event catalog. Plotted above this are lines that show swarms declared by the swarm tracking system (on this scale these lines are hard to see). Open circles show swarm escalations. B) The number of events per hour in the analyst-reviewed catalog. X marks explosive eruptions.

absolute value of D_{RS} in a one-minute time window. By taking the median, rather than the mean or the maximum value, noise spikes and short events are filtered out.

Redoubt began showing signs of unrest in September 2008, but it was not until 25 January 2009 that a significant increase in seismicity occurred (Figure 3). Following two months of vigorous steaming accompanied by volcanic tremor or modest earthquake swarms, explosive eruptions began on 23 March 2009. In the following weeks there were at least 19 explosive eruptions ejecting ash to altitudes of up to 20 km. These swarms and explosions were recorded on a 10-station network comprised of eight analog short-period stations and two digital broadband stations, supplemented by co-located infrasound from two sites. All stations were telemetered in real-time and used in the real-time event catalog.

We note five significant swarm episodes (Figure 4). The first occurred on 26–27 February and lasted about 32 hours. The second and most important began on 21 March culminating in the first explosive eruption on 23 March, lasting about 50 hours (Figure 5A). Others occurred on 27 March, 29 March and from 2–4 April (Figure 5B, C and D). These swarm episodes contained 815, 1,793, 410, 103, and 1,609 events respectively.

There were some clear differences in the behaviors of these swarm episodes. The event rate on 21–22 March rose gradually, but rose abruptly on 27 March and 29 March. The swarms on 23 March and 27 March merged into continuous tremor, and

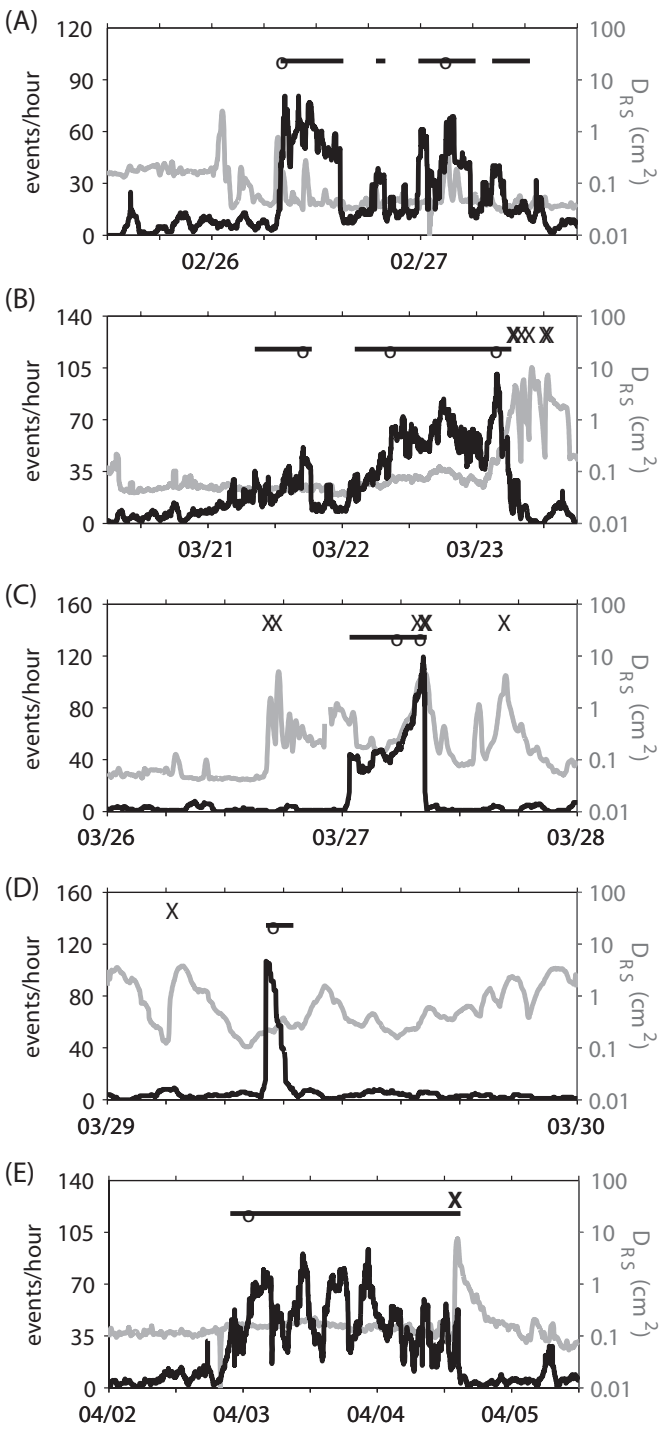

▲ **Figure 4.** Shown from top to bottom are the significant swarm episodes that occurred during unrest at Redoubt volcano in 2009. In each panel the black curve shows the median event rate (from the real-time catalog), the grey curve shows surface wave reduced displacement, D_{RS}. Black horizontal lines above these curves show the periods during which the swarm tracking system identified a swarm. Open circles superimposed on these lines represent escalation alarms. X along the very top marks explosive eruptions. The swarm episodes are from top to bottom: A) 26–27 February; B) 21–23 March; C) 27 March; D) 29 March; E) 2–4 April.

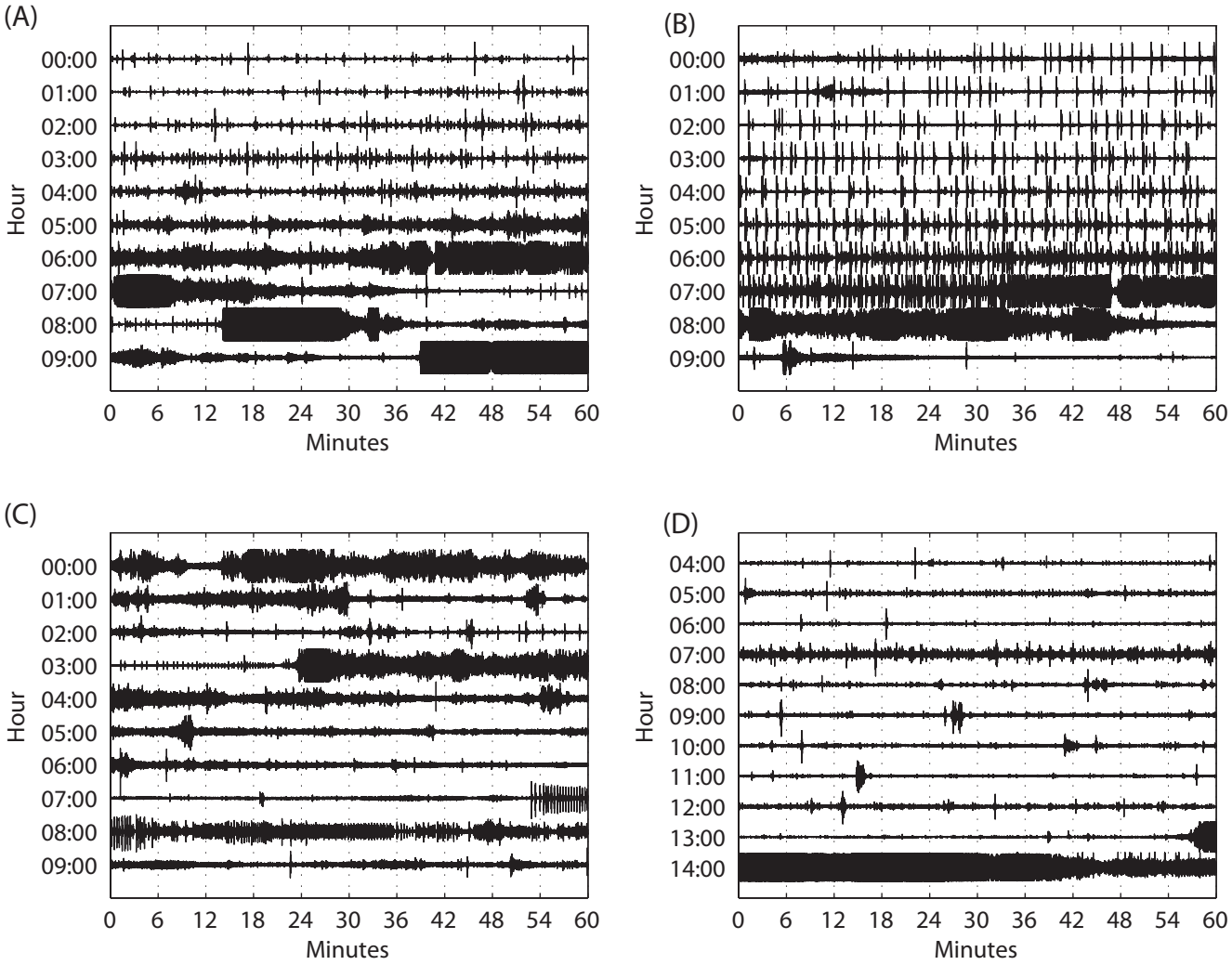

▲ **Figure 5.** Digital helicorder plots showing parts of the swarms on: A) 23 March; B) 27 March; C) 29 March; D) 4 April.

these swarms plus the one on 4 April culminated in explosive eruptions.

RESULTS

The thresholds used here reflect the specific seismic characteristics of Redoubt and the operational needs of AVO. After testing the swarm detection algorithm on archive data we settled on the following thresholds computed on a 60-minute time window. As we were interested in low-energy swarms, we did not use the magnitude parameters in our swarm criteria. The swarm_start threshold was *mean_rate* ≥ 16 and *median_rate* ≥ 32. The swarm_escalation threshold was *mean_rate* ≥ 24 and *median_rate* ≥ 48. The swarm_end threshold was *mean_rate* < 11 and *median_rate* < 22. The swarm_escalation and swarm_end thresholds are related to the swarm_start threshold by the significant change ratios for *mean_rate* and *median_rate*, which were both set at 1.5. The second-order swarm_escalation threshold was therefore *mean_rate* ≥ 36 and *median_rate* ≥ 72.

Applying these parameters to the catalog, four swarms (including two escalations) were identified on 26–27 February lasting 29 hours. (Figure 4A). Three other swarms were identified (on 22 February and 6 and 12 March), but averaged only 1 hour in duration (Table 1).

The first swarm of the explosive phase began on 21 March (Table 1). The event rate had increased gradually for about 11 hours, eventually crossing the threshold (Figure 4B). This upward trend continued and an escalation alarm was issued. There followed an abrupt decline in event rate, and an end of swarm alarm was issued 8.6 hours after the swarm was declared.

A second swarm was declared less than six hours later on 22 March. Two escalation alarms were declared indicating that the mean rate had surpassed 36 events per hour, and the median rate had surpassed 72. Figure 5A shows that this swarm continued to escalate until the events merged into tremor around 05:32. An alarm declaring the end of this swarm was issued 40 minutes later for a total swarm length of 28 hours. The first explosive eruption (since April 1990) began 25 minutes later at 06:38.

The 27 March swarm began at 00:45 and had two escalation alarms. Figure 5B shows that the swarm intensified and merged into tremor at around 07:40. Explosive eruptions occurred at 07:48, 08:29 and 08:43. There may also have been

TABLE I
Alarms declared. A total of 13 swarms and 35 alarms (13 start, 9 escalation and 13 end).

Alarm Time	Swarm State
22-Feb 10:36	swarm_start
22-Feb 12:13	swarm_end
26-Feb 07:54	swarm_start
26-Feb 08:05	swarm_escalation (Level 1)
26-Feb 15:08	swarm_end
26-Feb 18:53	swarm_start
26-Feb 19:57	swarm_end
26-Feb 23:44	swarm_start
27-Feb 02:54	swarm_escalation (Level 1)
27-Feb 06:19	swarm_end
27-Feb 08:13	swarm_start
27-Feb 12:34	swarm_end
06-Mar 12:10	swarm_start
06-Mar 12:53	swarm_end
12-Mar 13:54	swarm_start
12-Mar 14:35	swarm_end
21-Mar 08:21	swarm_start
21-Mar 16:58	swarm_escalation (Level 1)
21-Mar 18:34	swarm_end
22-Mar 02:14	swarm_start
22-Mar 08:38	swarm_escalation (Level 1)
23-Mar 03:33	swarm_escalation (Level 2)
23-Mar 06:13	swarm_end
27-Mar 00:45	swarm_start
27-Mar 05:37	swarm_escalation (Level 1)
27-Mar 07:59	swarm_escalation (Level 2)
27-Mar 08:38	swarm_end
29-Mar 08:06	swarm_start
29-Mar 08:29	swarm_escalation (Level 1)
29-Mar 09:30	swarm_end
01-Apr 17:26	swarm_start
01-Apr 18:25	swarm_end
02-Apr 21:42	swarm_start
03-Apr 01:01	swarm_escalation (Level 1)
04-Apr 14:51	swarm_end

an explosion around 08:02. The swarm_end was declared at 08:38. This example exhibits more latency than we would like at the end of swarms: the swarm_end was declared almost an hour following the onset of tremor.

Another good test of latency is the swarm on 29 March, which had an unusually abrupt onset at 07:52 (Figure 5C). The swarm_start alarm was issued at 08:06, a latency of 14 minutes. There had to be at least 16 events before the *mean_rate* threshold could be met. The swarm_end was declared at 09:30, a latency of 30 minutes.

The final swarm detected from 2–4 April lasted 41 hours and also revealed latency to be sub-optimal. The anticipated explosive eruption began at 13:58 (Figure 5D) but the swarm_end alarm was not issued until 14:51.

Overall we are encouraged by the results. A total of 13 swarms were detected from 10 October 2008 to 8 April 2009, and nine of these fell within the five main swarm episodes that occurred 26–27 February, 21–23 March, 27 March, 29 March and 2–4 April and generated a total of 27 alarms. These swarm episodes lasted an average of 25 hours.

The other four swarms detected occurred on 22 February, 6 March, 12 March, and 1 April and lasted an average of just 57 minutes.

DISCUSSION

The main criticism of the swarm tracking system must be the latency with which (mainly swarm_end) alarms were issued. The fundamental problem here is that the sensitivity of our system is related to the latency, as both depend on the length of the time window (maximum latency is the length of the time window). We used a time window of 1 hour, and with this 13 swarms were detected between 10 October 2008 and 8 April 2009. We reprocessed the event catalog but changed just one parameter—the length of the time window to 15 minutes. Had we used this parameter set, 130 swarms would have been detected, the vast majority of them less than 1 hour in duration. While this would have reduced latency to less than 15 minutes, an order of magnitude increase in alarms issued is not acceptable.

This is less of a problem than it initially appears. The main purpose of the swarm_end alarm is to signal the possibility that events have merged into continuous tremor, and this proved useful on 23 and 27 March for Redoubt volcano as swarms escalated into tremor and then explosive eruption. However, the goal of our system is to detect swarms, not eruptions. Systems can be designed for the latter. We ran a prototype tremor alarm system throughout the Redoubt crisis (in parallel with the swarm alarm system) and this successfully detected the escalations in volcanic tremor that preceded or coincided with most of the explosive eruptions (Thompson and West 2009). While there was no interaction between the swarm and tremor alarm systems, the same generic alarm manager and confirmation webpage was used.

This swarm detection algorithm is only as good as the event database it watches. With the parameters we have used, our theoretical event detection rate limit was about 300 events per hour. In practice the maximum event rate recorded was 120 events per hour (on 27 March). This was probably due to event codas overlapping on more distant stations first and there then not being enough network detections to declare an event. One way around this limitation is to use alternate event counting methods to create the catalog like single-station event detections or cross-correlation-based event detection (*e.g.,* Rowe *et al.* 2004). The first is wholly reliant on a single station of data and cannot provide location or magnitude information. The

second must be specifically tailored for a given dataset and will only detect certain families of events. Neither of these limitations are acceptable for our purposes. We prefer the robust and hands-free performance offered by a full event detection and location suite that makes use of the full network.

Our system is fully implemented in Antelope at this time, which allowed us to take advantage of its relational database structure, a deep data archive, and libraries in multiple programming languages which speed software development. However, we recognize that Earthworm is more widely used at volcano observatories and believe that our system design could be easily be reimplemented using Earthworm and MySQL. To calibrate the parameter settings for the swarm tracking logic, pre-existing knowledge of likely event detection rates is beneficial. Data from the 1989 Redoubt eruption allowed us to set reasonable thresholds. In the absence of *a priori* data, we would advise setting thresholds at low levels and then raising them if too many alarms result.

While alarm systems are not a substitute for a 24-hour operations room, if implemented well, they can play a vital role. Observatory scientists will sometimes miss what little precursory seismicity there is, or miss the onset of a major event. Operations rooms can be busy and stressful environments in which to work and it can be helpful to have alarm systems to objectively detect significant changes in activity that might otherwise go unnoticed in real-time. Given the rapid rate of human population growth in recent decades it seems likely that increasing numbers of people will live within range of active volcanoes, and more-sophisticated monitoring will be required to mitigate risk in balance with socio-economic needs. Integrated alarm systems will emerge, ingesting real-time data from different geophysical monitoring instruments (*e.g.,* seismic networks, lightning detection networks, infrasonic networks, and ground-based radar) providing better ways to detect (and locate) explosions, pyroclastic flows and ash columns.

DATA AND RESOURCES

The data used in this study are collected by the Alaska Volcano Observatory (a co-operative program between the United States Geological Survey, the Alaska Department for Geological and Geophysical Surveys, and the Geophysical Institute at the University of Alaska Fairbanks) as part of its routine monitoring operations.

ACKNOWLEDGEMENTS

We wish to thank Kent Lindquist for advice on Antelope internals and extending the schema.

REFERENCES

Aki, K., and R. Koyanagi (1981). Deep volcanic tremor and magma ascent mechanism under Kilauea, Hawaii. *Journal of Geophysical Research* **86**, 7,095–7,109.

Benoit, J. P., and S. R. McNutt (1996). *Global Volcanic Earthquake Swarm Database 1979–1989*. USGS Open File Report 96-69.

Benoit, J. P., G. Thompson, K. Lindquist, R. Hansen, and S. R. McNutt (1998). Near-realtime WWW-based monitoring of Alaskan volcanoes: The Iceweb system. *Eos, Transactions, American Geophysical Union* **79** (45), F957, *Fall Meeting Supplement* (abstract).

Bittenbinder, A. (1994). Earthworm: A modular distributed processing approach to seismic network processing. *Eos, Transactions, American Geophysical Union* **75** (44), 430.

Chouet , B. A., R. A. Page, C. D. Stephens, J. C. Lahr, and J. A. Power (1994). Precursory swarms of long-period events at Redoubt Volcano (1989–1990), Alaska: Their origin and use as a forecasting tool. *Journal of Volcanology and Geothermal Research* **62**, 95–135.

Hanks, T., and H. Kanamori (1979). A moment magnitude scale. *Journal of Geophysical Research* **84** (5), 2,348–2,350.

Harvey, D. J. (1999). Evolution of the Commercial ANTELOPE Software; http://www.brtt.com/docs/evolution.pdf

Lahr, J. C. (1989). *HYPOELLIPSE/Version2.0: A Computer Program for Determining Local Earthquake Hypocentral Parameters, Magnitude, and First Motion Patterns*. USGS Open-File Report 89-116, 92 pps.

Larsen, J., C. Neal, P. Webley, J. Freymueller, M. Haney, S. McNutt, D. Schneider, S. Prejean, J. Schaefer, and R. Wessels (2009). Eruption of Alaska volcano breaks historic pattern, *Eos, Transactions, American Geophysical Union* **90** (20), 173–174.

Marso, J. N., A. B. Lockhart, R. A. White, S. K. Koyanagi, F. A. Trusdell, and J. T. Camacho (2003). The Anatahan volcano monitoring system. *Eos, Transactions, American Geophysical Union* **84** (46), F1564.

Marso, J. N., T. L. Murray, A. B. Lockhart, and C. J. Bryan (2003). Glowworm, an extended PC-based Earthworm system for volcano monitoring (abs). In *Cities on Volcanoes 3: Hilo, Hawaii, International Association of Volcanology and Chemistry of the Earth's Interior (IAVCEI) Conference*, Hilo, Hawaii, 14–18 July 2003, abstract volume, p. 82.

McNutt, S. R. (1994). Volcanic tremor amplitude correlated with eruption explosivity and its potential use in determining ash hazards to aviation. In *Volcanic Ash and Aviation Safety: Proceedings of the First International Symposium on Volcanic Ash and Aviation Safety*, ed. T. J. Casadevall, 377–385. U.S. Geological Survey Bulletin 2047.

McNutt, S. R. (2002). Volcano seismology and monitoring for eruptions. In *International Handbook of Earthquake and Engineering Seismology*, part A, volume 81A, ed. W H. K. Lee, P. Jennings, C. Kisslinger, and H. Kanamori, Amsterdam and Boston: Academic Press.

Moran, S. C., S. D. Malone, A. I. Qamar, W. A. Thelen, A. K. Wright and J. Caplan-Auerbach (2008). Seismicity associated with renewed dome building at Mount St. Helens, 2004–2005. In *A Volcano Rekindled: The Renewed Eruption of Mount St. Helens, 2004–2006*, ed. D. R. Sherrod, W. E. Scott, and P. H. Stauffer, 27–50. USGS Professional Paper 1750.

Murray, T. L., and E. T. Endo (1992). A real-time seismic-amplitude measurement system (RSAM). In *Monitoring Volcanoes: Techniques and Strategies Used by the Staff of the Cascades Volcano Observatory, 1980–1990*, ed. J. Ewert and D. Swanson, 5-10. USGS Bulletin 1966.

Murray, T. L., J. A. Power, G. Davidson, and J. N. Marso (1996). A PC-based real-time volcano-monitoring data-acquisition and analysis system. In *Fire and Mud: Eruptions and Lahars of Mount Pinatubo, Philippines*, ed. C. G. Newhall and R. S. Punongbayan, 225–232. Quezon City: Philippine Institute of Volcanology and Seismology; Seattle: University of Washington Press.

Neuberg, J., R. Luckett, B. Baptie, and K. Olsen (2000). Models of tremor and low frequency event swarms on Montserrat. *Journal of Volcanology and Geothermal Research* **101**, 83–104.

Qamar, A. I., S. D. Malone, S. C. Moran, W. P. Steele, and W. A. Thelen (2008). Near-real-time information products for Mount St. Helens—tracking the ongoing eruption. In *A Volcano Rekindled: The Renewed Eruption of Mount St. Helens, 2004–2006*, ed. D. R. Sherrod, W. E. Scott, and P. H. Stauffer, 61–70. USGS Professional Paper 1750.

Robinson, M. R., C. A. Rowe, G. H. C. Sonafrank, and J. D. Davies (1991). XPick demonstration: Seismic analysis software system at the University of Alaska Geophysical Institute. *Seismological Research Letters* **62**, 23.

Rowe, C. A., C. H. Thurber, and R. A. White (2004). Dome growth behaviour at Soufriere Hills Volcano revealed by relocation of volcanic event swarms, 1995–1996. *Journal of Volcanology and Geothermal Research* **134**, 199–221.

Thompson, G., and M. E. West (2009). Alarm systems detect volcanic tremor and earthquake swarms during Redoubt eruption, 2009. *Eos, Transactions, American Geophysical Union Fall Meeting Supplement* (abstract).

Waythomas, C., S. Prejean, and S. R. McNutt (2008). Alaska's Pavlof volcano ends 11-year repose. *Eos, Transactions, American Geophysical Union* **89** (23); doi:10.1029/2008EO230002.

Weber, B., J. Becker, W. Hanka, A. Heinloo, M. Hoffman, T. Kraft, D. Pahlke, J. Reinhardt, J. Saul, and H. Thoms (2007). SeisComP3—automatic and interactive real-time data processing, *Geophysical Research Abstracts* **9**, 09219. http://www.cosis.net/abstracts/EGU2007/09219/EGU2007-J-09219.pdf

Geophysical Institute and Alaska Volcano Observatory
University of Alaska Fairbanks
903 Koyukuk Drive
Fairbanks, Alaska 99775, U.S.A.
gthompson@alaska.edu
(G.T.)

Appendix A—Cumulative Magnitude

The concept of cumulative magnitude (*cum_ml*) requires further elaboration. It is calculated using empirical relationships between local magnitude (M_L), seismic moment (M_0), and seismic energy (E_S) proposed by Hanks and Kanamori (1979):

$$\log_{10}(M_0) = 1.5\,M_L + 16.0 \quad (1)$$

and

$$E_S = M_0 / 2 \times 10^{-4} \quad (2)$$

Eliminating M_0 yields:

$$\log_{10}(E_S) = 1.5\,M_L + 11.7 \quad (3)$$

For each earthquake, energy is estimated using equation 3. The energy from each earthquake is then summed, and converted back to an equivalent local magnitude. The conversion factors of 16.0 in equation 1 and 11.7 in equation 3 assume that energy is measured in ergs. These should be changed to 9.0 and 4.7 respectively if energy is measured in Joules.